

Article

A Simulation Tool for Geometrical Analysis and Optimization of Fuel Cell Bipolar Plates: Development, Validation and Results

Alfredo Iranzo*, Felipe Rosa and Javier Pino

Department of Energy Engineering, University of Seville, Camino de los Descubrimientos s/n 41092 Seville, Spain; E-Mails: rosaif@us.es (F.R.) ; fjp@us.es (J.P.)

* Author to whom correspondence should be addressed; E-Mail: aip@esi.us.es; Tel.: +34-954-487471; Fax: +34-954-487247

Received: 1 July 2009; in revised form: 16 July 2009 / Accepted: 29 July 2009 /

Published: 31 July 2009

Abstract: Bipolar plates (BPs) are one of the most important components in Proton Exchange Membrane Fuel Cells (PEMFC) due to the numerous functions they perform. The objective of the research work described in this paper was to develop a simplified and validated method based on Computational Fluid Dynamics (CFD), aimed at the analysis and study of the influence of geometrical parameters of BPs on the operation of a cell. A complete sensibility analysis of the influence of dimensions and shape of the BP can be obtained through a simplified CFD model without including the complexity of other components of the PEMFC. This model is compared with the PEM Fuel Cell Module of the FLUENT software, which includes the physical and chemical phenomena relevant in PEMFCs. Results with both models regarding the flow field inside the channels and local current densities are obtained and compared. The results show that it is possible to use the simple model as a standard tool for geometrical analysis of BPs, and results of a sensitivity analysis using the simplified model are presented and discussed.

Keywords: fuel cell; simulation tool; bipolar plate; computational fluid dynamics

1. Introduction

Bipolar Plates (BPs) are very significant devices in the operation of fuel cells as final performance and cost will depend on the design of this component. The current design of BPs consists of rectangular section machined channels. One of the main functions of BPs is to distribute the reactant gases in a homogeneous way over the catalytic surface. Hence, channel dimensions and flow field designs have an important influence in the global efficiency of the cell. It is therefore necessary to analyse how the BPs geometry affects the performance of a fuel cell, in particular regarding pressure drop, water management and fuel consumption [1,2].

Software tools are widely used to evaluate the flow behaviour in the channels of BPs. In this paper, a simplified CFD model aimed to the analysis of geometrical influence of BPs in fuel cell is presented and validated against results provided by a more sophisticated tool, the PEMFC Module of the FLUENT software. This CFD tool models the electrochemistry, mass and current continuity, liquid water generation and transport, membrane humidification, electric losses, energy evacuation and other phenomena [3]. Therefore it constitutes an appropriate tool to validate the assumptions of the simplified model developed. The objective of this paper is to develop and present a methodology for the rapid performance evaluation, design and optimization of Bipolar Plates. The performance is evaluated according to fluid-dynamical considerations such as pressure drop and the plate ability to drag liquid water out of the cell, without the need for detailed resolution of FC phenomena occurring at the MEA. Therefore the advantage of full 3D fluid dynamical simulation is obtained without the penalty of resolving additional variables related to complex physics such as electrochemistry.

A validation study is also presented in order to verify that the simplified model is an appropriate tool to study how the BP design influences the PEMFC efficiency. Similar methodologies have been proposed in previous works, see for example Kumar and Reddy [4], although no validation was provided. The model is used to perform a sensitivity analysis of channel dimensions and flow field configurations, and the results obtained are discussed.

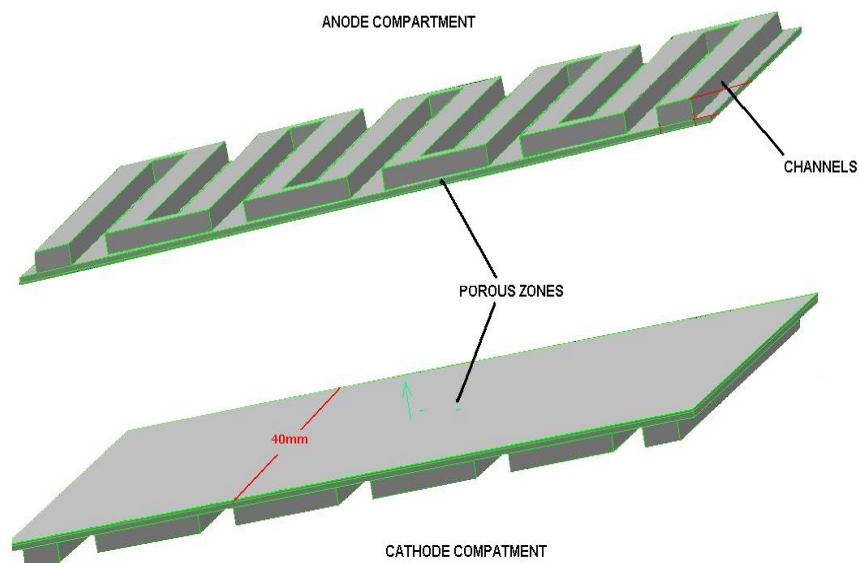
2. Solution Method and Model Description

The simplified CFD model is designed for steady state operation and isothermal conditions, and supplies information about the influence of BPs geometry without including the complex phenomena that occur in the MEA. The model solves the continuity and momentum equations and has been successfully used to optimize BPs' geometry [5,6].

In order to compare the results from the developed simplified model and the FLUENT PEMCF Module, a bipolar plate design have been established and solved with both software tools. The geometry and dimensions of the bipolar plate are shown in Figure 1, where the geometry for the simplified model has been represented for the anode and cathode sides. Both BPs have the same configuration and dimensions. The active surface area is $40 \times 40 \text{ mm}^2$, with ten channels in a serpentine flow field configuration. The channels are 2 mm in width and 1 mm in depth. The width of

the rib is 2 mm. The thickness of the porous zones is 0.354 mm, which is equivalent to the thickness of the gas diffusion layer and the catalytic layer according to [7].

Figure 1. Simplified geometry model of the bipolar plate for anode and cathode sides.



2.1. Model Assumptions

The simplified model is based on two main assumptions:

First, that the current density generated in anode side is proportional to the hydrogen velocity in the consumption direction in the anode catalytic layer. This assumption allows for the calculation of the distribution of current density over the anode electrode surface, from the gas velocity distribution.

Secondly, that the current density generated in both sides (anode and cathode) are identical for corresponding locations in the anode and cathode catalytic layers. This assumption is used to calculate the current density of cathode side.

The methodology used to perform an analysis is the following. First, the anode side model is created and solved, and the gas velocity in the consumption direction at the electrode surface is stored and used to calculate the corresponding oxygen consumption in the cathode side model [5,6]. Here, the described model assumptions are used. Then, the cathode side model is defined with the calculated boundary conditions and finally solved. By using this approach, parametric analysis and BPs geometry optimization can be performed in a straightforward manner.

2.2. Governing Transport Equations

The Finite Volume Method is used to resolve the complete set of Navier-Stokes equations governing the fluid flow motion. The general form of the transport equation is given by:

$$\frac{\partial}{\partial t} \int_V \rho \phi dV + \oint_A \rho \phi V \cdot dA = \oint_A \Gamma \nabla \phi \cdot dA + \int_V S_\phi dV \quad (1)$$

where ϕ is the transported quantity. The first term in the equation corresponds to the transient transport of ϕ , the second term to the transport by convection mechanism, the third term represents the transport of ϕ by diffusion, and the fourth term represents the source (or sink) or generation of ϕ . The different transport equations are assembled by using the appropriate variables (Table 1).

Table 1. Transport equations used in the CFD analysis.

Equation	Variable ϕ
Continuity	1
x-momentum	U
y-momentum	V
z-momentum	W
Chemical species i	y_i

Therefore, the mass conservation or continuity equation is given by substituting ϕ in Equation 1 by 1. The momentum conservation equations in x, y, z direction is given by substituting ϕ in Equation 1 by u, v, w, which are the fluid velocity in each space direction. The chemical species conservation equation is given by substituting ϕ in Equation 1 by y_i , which is the mass fraction of specie i representing the water vapour content in the reactant gases.

There are source terms in the above equations arising from the pressure difference of the fluid flowing through the porous media. The modelling of flow in porous media is a key issue in fuel cells, as both GDL and catalytic layer are porous materials. Typically, the porous media is represented by adding a negative source in the momentum equations, so that a pressure drop is generated accordingly. The source term is in general decomposed in two parts as in Equation 2, the first one representing the viscous loss as in Darcy's law, and the second one representing inertial losses:

$$S_i = - \left(\frac{\mu}{\alpha} v_i + C_2 \frac{1}{2} \rho v_{mag} v_i \right) \quad (2)$$

where α is the permeability of the porous material, μ and ρ are the dynamic viscosity coefficient and the flow density respectively. C_2 is the inertial resistance of the zone and v_i is the flow velocity in the i-direction.

For the velocity ranges typically found in fuel cell GDL and catalytic layers only the viscous loss is significant and therefore only this term has been considered in the model. The porous zone is assumed to be isotropic, with viscous resistance ($1/\alpha$) of 10^{12} m^{-2} .

2.3. Anode Compartment Model

The base case for the validation work consists of an anode BP model and the corresponding cathode BP model, with a serpentine flow field design with one inlet and one exit, and 1 mm width channels.

Below the channels a porous zone (GDL or Gas Diffusion Layer) with a viscous resistance is modelled. The outlet of the GDL region, corresponding to the catalytic layer, accounts for the hydrogen consumption by imposing the gas consumption. The layer thickness and transport properties are defined according to the values reported by Um and Wang [7] and Natarajan and Van Nguyen [8].

Using this model as a base case a detailed analysis of the geometry of the BP can be performed, as different modifications of the flow-field design can be compared (serpentine, parallel, pin type, etc.) The effect of varying the dimensions of the channels and ribs can also be analysed.

2.4. Cathode Compartment Model

The model for the cathode side is geometrically identical to the anodic model. However, boundary conditions are different and new physical phenomena such as water removal and multiphase flow must be considered. The cathode side model consists of three main control volumes: channels, GDL and catalytic layer. GDL and catalytic layer are included in order to model oxygen consumption and water production [9]. The layer thickness and transport properties are defined according to the values reported by Um and Wang [7] and Natarajan and Van Nguyen [8].

2.5. Boundary Conditions

Anode consumption and anode channel inlet: For validation purposes the anode reactant consumption and channel inlet mass flows are calculated according to typical operating conditions. Current density of PEM fuel cells varies between 2,000 A/m² and 7,000 A/m². In order to determine the consumption an average current density of 5,000 A/m² is imposed, and using an experimental polarization curve a voltage of 0.64 V has then been established. The power density of the cell is therefore 3.78 kW/m². Currently a typical PEM fuel cell requires around 1.0 Nm³ of pure hydrogen to produce 1.8–1.9 kW, while around 30% or 40% is lost in the operation. Thus, a hydrogen consumption of 1.05×10^{-7} kg/s is considered. It is established that all the hydrogen entering in the cell is consumed, so 1.05×10^{-7} kg/s of hydrogen must be introduced. By using a psychometric chart of the hydrogen-water vapour mixture the absolute humidity depending on the inlet temperature is obtained, obtaining the gas mixture mass flow at the anode inlet, 2.36×10^{-7} kg/s.

Cathode consumption and cathode channel inlet: The oxygen consumption rate is calculated from the hydrogen consumption densities calculated in the analysis of the anodic compartment. By applying the overall reaction that takes place on the catalytic layer, the according stoichiometric consumption densities of oxygen are obtained. The quantity of necessary humidified air to consume the stoichiometric oxygen is then calculated. An excess of 2.5 of oxidizing gas at the inlet is imposed, a value typically used for ensuring water removal.

Liquid water generation: In order to model the water removal without including the complex physical phenomena within the cell, the liquid water generated is imposed to appear over the channel-GDL

interface, and it is defined as a volumetric source of liquid water proportional to the oxygen consumption rate.

3. Model Validation

As described in Section 2, the simplified model has been developed using two main assumptions. In this section, this model is compared against the PEM Fuel Cell Module of FLUENT in order to verify the appropriateness of the assumptions.

The first assumption considers that the current density is proportional to the gas velocity in the consumption direction over the anode-electrode surface. This assumption means that the relation between current density and velocity (in the consumption direction) does not depend on the position in the plane (x,y). Thus:

$$i_e(x, y, z_0) = K(x, y, z_0)v_z(x, y, z_0) \xrightarrow{\text{yields}} K(x, y, z_0) = \text{constant} \cdot \forall(x, y, z_0) \quad (3)$$

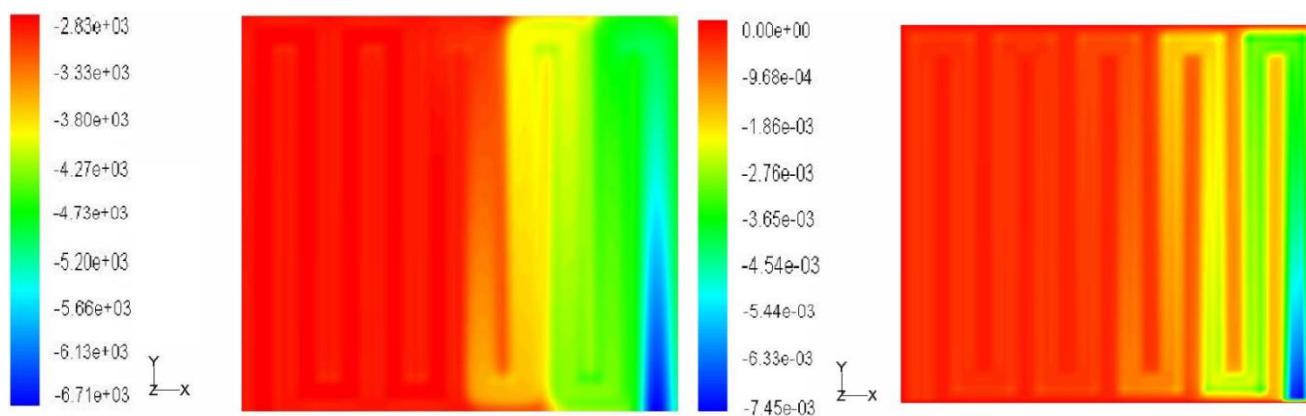
where i_e is the current density (A/m^2), v_z is the mixture velocity in the z-direction (m/s), z_0 is the coordinate in the z axis related to the anode catalytic layer (through-plane coordinate).

In order to verify this a magnitude $K(x,y)$ is created in the FLUENT PEMFC Module results, and defined as the ratio between the current density in the anode catalytic layer i_e and the gas velocity in the consumption direction v_z . Therefore $K(x,y)$ should be constant for all the points (x,y) on the working surface of the electrode:

$$K(x, y, z_0) = i_e(x, y, z_0)/v_z(x, y, z_0) \quad (3)$$

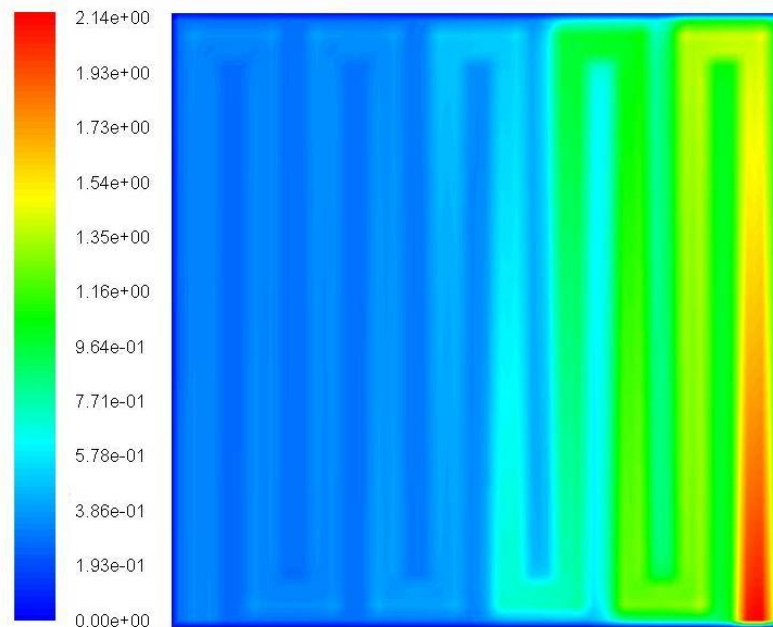
Figure 2 shows the distribution of both magnitudes over the electrode surface. The current density distribution -at the left- shows that most of the consumption starts in the middle of the hydrogen path until the outlet. Something similar can be noticed in the gas velocity distributions.

Figure 2. Distribution of current density (left) and z-velocity (right) over the anode electrode surface. Results from the FLUENT PEMFC Module.



The distribution of $K(x,y)$ divided by its mean value over the surface (K/K_m) is represented in Figure 3. An important dependency of $K(x,y)$ with the location is observed, especially at the inlet zone. Therefore it is not possible to affirm that the assumption is valid, but as can be seen in Figure 3, velocities over the consumption surface are in general an excellent parameter to analyse the utilisation of the whole area of MEA.

Figure 3. Distribution of $K(x,y)/K_m$ over the anode electrode surface. Results from the FLUENT PEMFC Module.



The second assumption is used to calculate the real oxygen consumption on the cathode compartment. The oxygen consumed locally can be calculated from local current density over anode electrode surface, as it is established that distributions on both the anode and cathode electrode surfaces are identical:

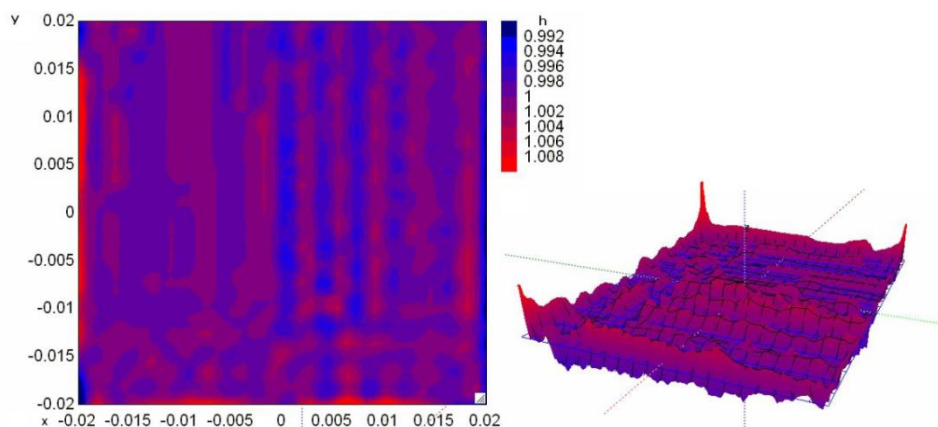
$$i_{e,a}(x_a, y_a, z_a) = i_{e,c}(x_c, y_c, z_c) \quad (4)$$

where $i_{e,a}$ is the local current density over the anode electrode and $i_{e,c}$ is the local current density over the cathode electrode. In order to verify this, the current densities in both surfaces are calculated using the PEMFC Module of FLUENT, and the function $h(x,y)$ is created and defined as the ratio between the anode current density and the cathode current density:

$$h(x, y) = \frac{i_{e,a}(x_a, y_a, z_a)}{i_{e,c}(x_c, y_c, z_c)} \quad (5)$$

The values of h for every location (x,y) must be the unity. Figure 4 represents this magnitude. Maximum and minimum values are 1.008 and 0.992, respectively. Hence, it is verified that for every point of the active surface, the values of current densities in both electrode surfaces, can be considered to be identical.

Figure 4. Distribution of $h(x,y)$ over the anode electrode surface. Results from the FLUENT PEMFC Module.



Finally it is also necessary to ensure that both models provide the same velocity profiles in the anode electrode surface. In order to perform this analysis the function $q(x,y)$ is defined in the FLUENT PEMFC Module results as the relation between both velocities in consumption direction:

$$q(x,y) = \frac{v_z(x,y,z_a)|model}{v_z(x,y,z_c)|FLUENT_PEMFC_Module} \tag{6}$$

This function has to be as close to the unity as possible to affirm that the assumption is correct.

Figure 5. Contours lines of $q(x,y)$ over the electrode surface. Results from the FLUENT PEMFC Module.

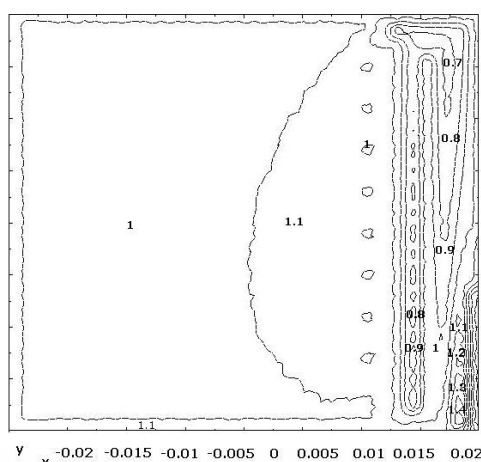


Figure 5 represents the distribution of $q(x,y)$ over the surface, showing limit values up to 1.4 and 0.6. In principle this means that velocity profiles are different, but the lines “iso-values” of $q(x,y)$ represented in Figure 5 shows that for most of the locations, both velocity distributions are mainly identical. Only at the zone close to the inlet the values of $q(x,y)$ differ from the unity, probably caused by the non fully-developed condition used for the simplified model.

4. Model Results

It has been shown that the simplified model is an appropriate approach for the analysis of bipolar plates. The model has been used for geometry optimization and sensitivity analysis and the results are presented and discussed in this section. Different flow field designs and channel dimensions have been considered. In Figure 6 some of these flow field designs are shown, and Table 2 shows a detailed description of the cases analysed.

Figure 6. Different flow field designs studied in the sensitivity analysis.

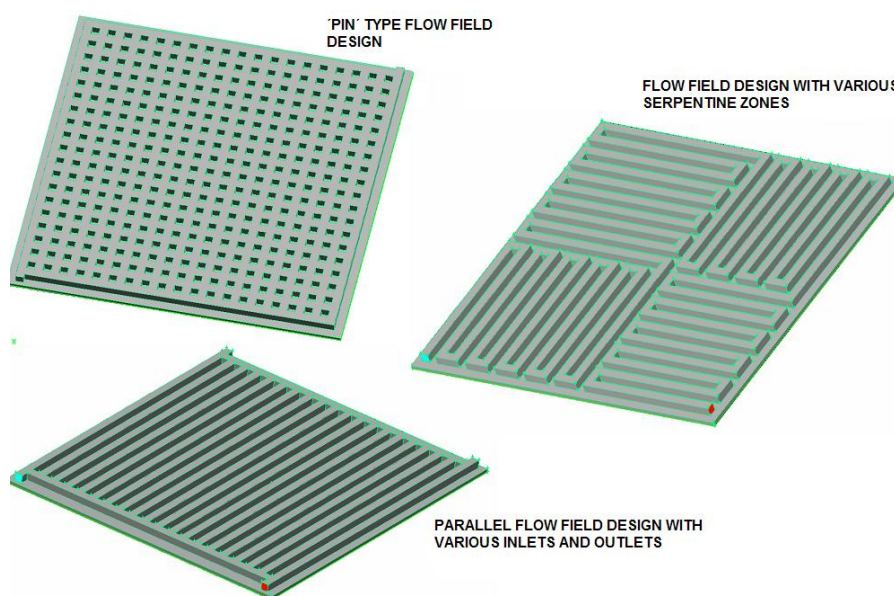


Table 2. Description of the configurations studied in the sensitivity analysis.

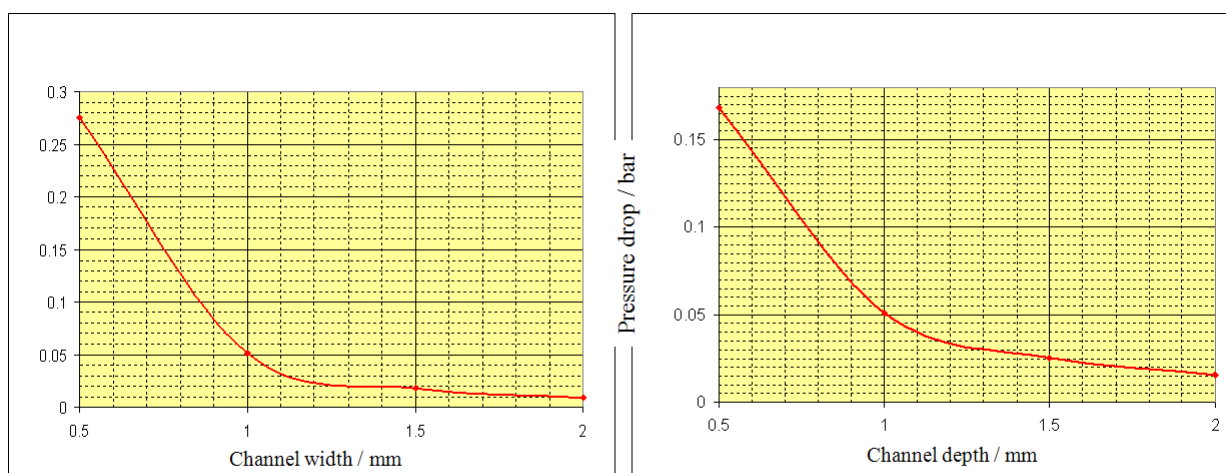
Case ID	Flow field design	Channel width (mm)	Channel depth (mm)	Number of channels
Base case	Serpentine	1	1	20
Case 2	Serpentine	0.5	1	27
Case 3	Serpentine	1.5	1	16
Case 4	Serpentine	2	1	13
Case 5	Serpentine	1	0.5	20
Case 6	Serpentine	1	1.5	20
Case 7	Serpentine	1	2	20
Case 8	Serpentine	1	1	20
Case 9	Parallel	1	1	20
Case 10	Parallel with various inlet/outlets	1	1	40
Case 11	Various serpentine zones	1	1	-
Case 12	“Pin” type	1	1	-

4.1. Sensitivity Analysis of Channel Dimensions

First, the effect of the main channel dimensions have been studied by comparing the results obtained from the different cases with the base case.

In particular, results from cases 2, 3 and 4 can be compared with the base case in order to analyse the effect of the channel width. Figure 7a shows the pressure drop of the reactant gas, where an increase of channel width leads to a decrement of the pressure drop. The same effect occurs for models 5, 6 and 7, where the varied parameter is the channel depth. Figure 7b shows the pressure drop for different channel depths, and pressure drop also decreases with the increase of channel dimensions. Therefore, increasing the channel dimensions results in a better performance of the stack, in terms of reactant pressure drop. However, an appropriate design must consider both pressure drop and water removal capabilities, so pressure drop alone is not a design variable where a design can be based. Typically, a higher pressure drop involves an improved water removal, as liquid water will be more effectively dragged by a larger pressure gradient in the gas phase. The BP flow field design must be based on a compromise aiming at reducing the pressure drop and enhancing the water removal.

Figure 7. Pressure drop for cases varying channel width (a) and channel depth (b).

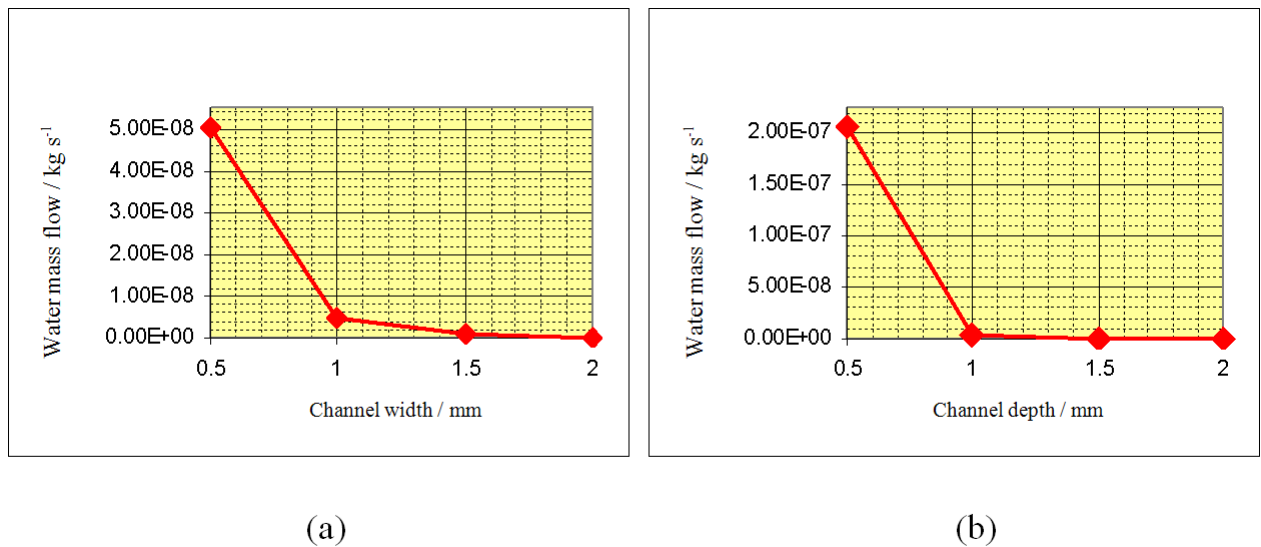


(a)

(b)

For that reason, it has been studied how the geometry of the plates influences the dragging of the liquid water by the reactant gases. Figure 8 shows the influence on the channel width (a) and the channel depth (b). For both geometrical parameters the effect is similar: the smaller the channel dimensions, the better the water extraction. This conclusion is clearly related to the previous results about pressure drop.

Figure 8. Water removal for cases varying channel width (a) and channel depth (b).



4.2. Sensitivity Analysis of Different Geometrical Configurations

Figure 6 shows some of the analysed plates, which are described in Table 2. Cases 9, 10, 11, 12 are compared against the base case. In Table 3 the pressure drop for each case can be seen. Both serpentine flow field designs are the geometrical configurations where the pressure drop is larger. For parallel designs the pressure drop is lower, and for an increase in the number of inlets and outlets the pressure drop is even lower. However, the best configuration according to pressure drop is the “pin” type configuration, where the pressure drop achieves the lowest value.

Table 3. Pressure Drop for different flow field configurations.

Case	Flow field design	Pressure drop (bar)
Base case	Serpentine	0.0510
Case 9	Parallel	0.0031
Case 10	Parallel with various inlet/outlets	0.0029
Case 11	Various serpentine zones	0.0628
Case 12	“Pin” type	0.00057

The water removal capability of each plate is shown in Table 4. The effect of including various inlets and outlets as in cases 10 and 11 leads to an increase of the removed water. Another effect observed is that the quantity of removed water in the design with various serpentine zones is less than the removed quantity in the simple one. According to the results obtained, the design with the best water removal capability is the “pin” type configuration. However, it is well known [1] that a pin

design flow field typically presents channelling effects, formation of stagnant areas, uneven reactant distribution, and inadequate water removal. This is because reactants flowing through such flow fields tend to follow the path of least resistance, leading to a minimal pressure drop but also to poor water removal. Therefore, this particular result obtained for the pin type configuration must be reconsidered and further analysed as it does not reproduce the typical behaviour observed in such BPs.

Table 4. Water removal capability for different flow field configurations.

Case	Flow field design	Removed water (kg/s)
Base case	Serpentine	4.77×10^{-9}
Case 9	Parallel	1.19×10^{-10}
Case 10	Parallel with various inlet/outlets	9.57×10^{-10}
Case 11	Various serpentine zones	5.13×10^{-10}
Case 12	“Pin” type	1.58×10^{-8}

5. Conclusions

The objective of this paper was to validate the simplified CFD fuel cell model that was developed. The model is aimed to analyse the influence of the geometry and dimension of BPs in the operation of the cell. The way to verify the accuracy and feasibility of this model consists of ensuring that the used hypotheses are correct, and in order to analyse these hypotheses the Model of PEM fuel cell of Fluent is used.

The results shows that the simplified model provide the same velocity profiles than the PEMFC Model implemented in FLUENT, with some differences in the zones close to the channel inlet. The second assumption of equality of current density distribution has been also correctly verified. However, it is not possible to validate the first assumption. The analysis of the relation between current density and velocity in consumption direction reveals that this magnitude is not constant in every point of the electrode surface. Despite this, the model can be used with confidence for the analysis of the influence of the geometry of the BPs, and the velocity distribution over the anode electrode surface is an appropriate index to evaluate the homogeneity of the use of the area of the MEA.

According to the results obtained with the simplified model for different BPs geometries, reduced channel dimensions increases pressure drop and improve water removal. Various flow field designs of plates have been tested. The serpentine flow field design is in general less favourable, and it can be observed that including various inlets and outlets decreases the pressure drop and improves water management.

Acknowledgements

This work is part of the project P08-TEP-4309 Experimental Validation of a Methodology for the Development of PEM Bipolar Plates, funded by Junta de Andaluc ía. In addition, authors would like to

acknowledge the close collaboration with the National Institute for Aerospace Technology (INTA) in the field of PEMFC CFD modeling and experimental validation.

References and Notes

1. Li, X.; Sabir, I. Review of bipolar plates in PEM fuel cells: Flow-field designs. *Int. J. Hydrogen Energy* **2005**, *30*, 359–371.
2. Sun, W.; Peppley, B.A.; Karan, K. Modeling the Influence of GDL and flow-field plate parameters on the reaction distribution in the PEMFC cathode catalyst layer. *J. Power Sources* **2005**, *144*, 42–53.
3. *FLUENT 6.2 Documentation*; Fluent Inc.: Lebanon, NH, USA, 2005.
4. Kumar, A.; Reddy R.G. Effect of channel dimensions and shape in the flow-field distributor on the performance of polymer electrolyte membrane fuel cells. *J. Power Sources* **2003**, *113*, 11–18.
5. Martínez, J.J.; Pino, F.J. Sensitivity analysis of the design parameters of cathode side of the bipolar plates. In *Proceedings of the 16th World Hydrogen Energy Conference*, Lyon, France, June 2006; p. 117.
6. Martínez, J.J.; Rosa, F.; Pino, F.J. Sensibility analysis of design parameters of bipolar plates in PEM fuel cells. In *Proceedings of the 2nd European Hydrogen Energy Conference*, Zaragoza, Spain, November 2005; p. 578.
7. Um, S.; Wang, C.Y. Three-dimensional analysis of transport and electrochemical reactions in polymer electrolyte fuel cells. *J. Power Sources* **2004**, *125*, 40–51.
8. Natarajan, D.; Van Nguyen, T. Three-dimensional effects of liquid water flooding in the cathode of a PEM fuel cell. *J. Power Sources* **2003**, *115*, 66–80.
9. Pasaogullari, U.; Wang, C.Y. Liquid water transport in gas diffusion layer of polymer electrolyte fuel cells. *J. Electrochem. Soc.* **2004**, *151*, A399–A406.

© 2009 by the authors; licensee Molecular Diversity Preservation International, Basel, Switzerland. This article is an open-access article distributed under the terms and conditions of the Creative Commons Attribution license (<http://creativecommons.org/licenses/by/3.0/>).